A theoretical study of atmospheric pollutant NO_2 on as-doped monolayer WS_2 based on DFT method

Hou, Shuhan; Wang, Zhaokun; Yang, Huiru; Jiang, Jing; Gao, Chenshan; Liu, Yufei; Tang, Xiaosheng; Ye, Huaiyu

DOI
10.1016/j.physe.2022.115446

Publication date
2022

Document Version
Final published version

Published in
Physica E: Low-Dimensional Systems and Nanostructures

Citation (APA)
Hou, S., Wang, Z., Yang, H., Jiang, J., Gao, C., Liu, Y., Tang, X., & Ye, H. (2022). A theoretical study of atmospheric pollutant NO_2 on as-doped monolayer WS_2 based on DFT method. *Physica E: Low-Dimensional Systems and Nanostructures*, *144*, Article 115446. https://doi.org/10.1016/j.physe.2022.115446

Physica E 144 (2022) 115446

Contents lists available at ScienceDirect

Physica E: Low-dimensional Systems and Nanostructures

journal homepage: www.elsevier.com/locate/physe

A theoretical study of atmospheric pollutant NO_2 on as-doped monolayer WS_2 based on DFT method

Shuhan Hou [a,1], Zhaokun Wang [a,1], Huiru Yang [a,b], Jing Jiang [c], Chenshan Gao [a], Yufei Liu [d], Xiaosheng Tang [e], Huaiyu Ye [a,f,*]

[a] School of Microelectronics, Southern University of Science and Technology, Shenzhen, 518055, China
[b] Harbin Institute of Technology, Harbin, 150001, China
[c] Academy for Engineering & Technology, Fudan University, Shanghai, 200433, China
[d] College of Optoelectronic Engineering, Chongqing University, Chongqing, 400044, China
[e] College of Optoelectronic Engineering, Chongqing University of Posts and Telecommunications, Chongqing, 400065, China
[f] Electronic Components, Technology and Materials, Delft University of Technology, 2628 CD Delft, the Netherlands

A B S T R A C T

For the relevant properties of pristine and doped (Si, P, Se, Te, As) monolayer WS_2 before and after the adsorption of CO, CO_2, N_2, NO, NO_2 and O_2, density functional theory (DFT) calculations are made. Calculation results reveal that the monolayer WS_2 doped with P and As atoms can be substrate materials for NO and NO_2 gas sensors. However, after the subsequent CDD and ELF calculations, it is found that P-doped monolayer WS_2 adsorbs NO and NO_2 in a chemical way, while As-doped monolayer WS_2 adsorbs NO and NO_2 in a physical way. Also, the charge transfer between As-doped monolayer WS_2 and NO is relatively small and not easily detected. Besides, As-doped monolayer WS_2 system exhibits greater differences in optical properties (the imaginary part of reflectivity and dielectric function) before and after the adsorption of NO_2 gas than before and after adsorption of NO gas. These differences in optical properties assist sensor devices in making gas adsorption-related judgments. Through the analysis of the recovery time, DOS and PDOS, As-doped monolayer WS_2 is also verified to be a promising NO_2 sensing material, whose recovery time is calculated to be as short as 0.169 ms at 300 K.

1. Introduction

Gases are diverse and ubiquitous. Usually, different gases have different properties and sources. For instance, some gases are indicators of life and health, while others are highly dangerous or even deadly. One of the most common samples of harmful gases is NO_2, which can be widely seen in both chemical synthesis and industrial production. It is reported that when the concentration of NO_2 in our surrounding environment exceeds 1 ppm, severe respiratory diseases can be caused [1]. Toxic gases like NO_2 not only harm the human body, but also give rise to severe environmental issues, for instance, acid rain and photochemical smog [2,3]. Thereby, gas sensing is needed in various fields represented by environmental protection and safety monitoring of industrial processes [4]. Besides, detection of toxic gases is also crucial for the maintenance of air quality, the control of vehicle emissions, medical diagnosis and biohazard detection [5–8]. The leakage of these gases must be closely monitored.

Metal oxide gas sensors have once been widely concerned, but they were found having the defects of instability and limited working conditions [9]. Therefore, we need to search for new materials that can be used for the detection of these gases [10]. In order to detect gas molecules as efficiently as possible, it is essential that the material has a large surface-to-volume ratio and the ability of providing binding force which is sufficient enough for gas adsorption [11,12]. Two-dimensional (2D) materials, like graphene [13], just meet the above requirements. They have a high surface-to-volume ratio, a wide range of chemical compositions, and a unique thickness dependence [14,15]; all these characteristics make 2D materials ideal for applications in the field of gas sensing. Researches also reveal that 2D materials exhibit excellent properties and performance in nano electronic devices [16,17], and that 2D materials-based gas sensors have higher sensitivity, selectivity, response and recovery rate, and stability [18]. Consequently, 2D materials have been extensively studied for the past few years.

It is worth mentioning that, in particular, compared with graphene and other 2D materials, 2D transition metal dichalcogenides (TMDs) display obvious advantages in performance whether they are used as substrate materials for electronic, optical or electrochemical sensors [19–23]. Latest researches have concentrated on two TMDs: MoS_2

* Corresponding author. School of Microelectronics, Southern University of Science and Technology, Shenzhen, 518055, China.
E-mail address: yehuaiyu@gmail.com (H. Ye).
[1] These authors contributed equally to this work.

https://doi.org/10.1016/j.physe.2022.115446
Received 11 January 2022; Received in revised form 5 June 2022; Accepted 20 July 2022
Available online 30 July 2022

[24–27] and WS_2 [28,29]. Both theoretical and experimental studies have shown that MoS_2 nanosheets are sensitive detectors for NO, NO_2, NH_3 and triethylamine gases [24,26,30–34]; but the gas sensing performance of WS_2 nanosheets has been seldom studied. In fact, as a member of TMDs materials, WS_2 has a variety of unique characteristics of sensing materials [35,36]. In 2015, the charge transfer of gas molecules adsorbed on 2D WS_2 was theoretically investigated [37]. What they have found is that most gas molecules (such as H_2, O_2, H_2O and NH_3) can be adsorbed on the surface of WS_2 monolayer in a physical way, which indicates that WS_2 is indeed promising as a gas sensing material.

In this study, the adsorption of NO_2 and five other common gases (CO, CO_2, N_2, NO, O_2) on 2D WS_2 is systematically investigated through first principal calculations, so as to explore the possibility of 2D WS_2 as a substrate material for NO_2 sensors. Considering that the pristine 2D sensing material has poor adsorption capacity for the target gas, that is, it cannot effectively capture gas molecules [38]; in order to modify the binding forces between the material and the gas molecules, and to enhance the sensing capabilities of materials, doping is widely applied throughout the research of 2D materials [39,40]. For instance, in gas sensing, Pd-doped WS_2 exhibits obvious merits over the pristine WS_2 [7,41]. And since P, Si, Se, Te and As atoms have a covalent radius close to that of S atoms, the S atom can be easily replaced by them and a stable covalent structure at the doping site can be formed [42–45]. Therefore, we investigate the adsorption effect of P, Si, Se, Te and As doped WS_2 on NO_2 and the above five gases. In addition, we also examine the extent to which the sensing performance of the 2D WS_2 is affected when exposed to the atmosphere. This work provides a comprehensive insight into the application of 2D WS_2 for NO_2 gas sensing.

2. Methodology

First-principle calculations are carried out substrated on the framework of DFT [46–48]. The exchange correlation interaction is processed via the generalized gradient approximation (GGA) within the Perdew-Burke-Ernzerh (PBE) functional [49,50]. To better describe the interlayer van der Waals (vdW) interactions, the dispersion corrected density functional theory (DFT-D) [51] with Grimme [52] methods is applied. All of the atomic positions are optimized until the force and the energy tolerances are below 0.002 Ha/Å and 10^{-5} eV, respectively. The Brillouin zone integration is sampled for a 3×3 WS_2 supercell using $5 \times 5 \times 1$ and $9 \times 9 \times 1$ k-grid meshes so as to calculate the geometry optimization and electronic properties, respectively;

The adsorption energy (*Ea*) is obtained through the following formula to intuitively reflect the adsorption strength between WS_2 and gas molecules:

$$Ea = E_{WS_2+gas} - E_{WS_2} - E_{gas} \quad (1)$$

where $E_{WS2+gas}$, E_{WS2} and E_{gas} stand for the overall energy of the system composed of monolayer WS_2 and the adsorbate, the energy of monolayer WS_2, and the energy of the isolated gas molecule, respectively. Besides, to explore the electron redistribution in these systems, the charge density difference (CDD) is calculated via:

$$\Delta\rho = \rho_{WS_2+gas} - \rho_{WS_2} - \rho_{gas} \quad (2)$$

where $\rho_{WS2+gas}$, ρ_{WS2} and ρ_{gas} stand for the charge density of the system composed of monolayer WS_2 and the adsorbate, the charge density of monolayer WS_2, and the charge density of the isolated gas molecule, respectively. To precisely estimate the interaction mechanism between monolayer WS_2 and gas molecules, the electron localization function (ELF) of some systems is also considered.

3. Results and discussion

To begin with, calculation results of the geometry optimization are examined: the lattice constants a and b of the WS_2 unit cell are both equal to 3.242 Å, which are in accordance with the values obtained by other research groups [53].

3.1. Structural characteristics of WS_2 monolayer

Fig. 1 demonstrates that monolayer WS_2 is composed of three layers of atoms. For the S atoms in the uppermost and lowermost layers, they are each bonded to three W atoms; while for the W atoms in the interlayer, they are each bonded to six S atoms. As for possible adsorption positions on monolayer WS_2, there are three possibilities, which are P1 (on top of a S atom), P2 (on top of a W atom), and P3 (on top of the center of the W–S–W–S–W–S hexatomic ring).

3.2. Adsorption of gas molecules on WS_2 monolayer

To probe the sensing behavior of monolayer WS_2 for gas molecules (CO, CO_2, N_2, NO, NO_2, O_2), we calculate different structural and electrical characteristic parameters of different adsorption systems. The initial distance between monolayer WS_2 and the gas molecule is set to 3.00 Å. Among these parameters, *d* represents the shortest distance between the atoms of monolayer WS_2 and the adsorbed gas molecule, while *r* is the related covalent radii. The charge transfer (ΔQ) is calculated by means of Mulliken population analysis. The negative value of ΔQ indicates that the charge transfers from monolayer WS_2 to the gas molecule. More detailed calculation results are given in Table 1.

As shown in Table 1, except for the NO and NO_2 adsorption systems, no charge transfer exists between monolayer WS_2 and the gas in the other four adsorption systems. However, the ΔQ of the NO and NO_2 adsorption systems are merely 0.04 e and 0.03 e respectively, which is almost negligible. To make matters worse, the *d* in each adsorption system is also greater than the initial value (3.00 Å). Even in the NO/WS_2 system with the smallest *d*, the difference between *d* and *r* is as much as 1.43 Å. The above facts all indicate that the interaction between the pristine WS_2 monolayer and the gas may not be strong.

In order to verify our guess, we selectively calculate the CDDs and ELFs of the NO and NO_2 adsorption systems. The reason for choosing these two systems is that in these two systems, there is at least certain charge transfer between the substrate and the gas. As expected, as displayed in Fig. 2, from the CDDs of the two systems (Fig. 2(a, b, d, e), we can see that there is almost no charge accumulation and depletion between monolayer WS_2 and the gas. Besides, the ELFs (Fig. 2(c, f)) also

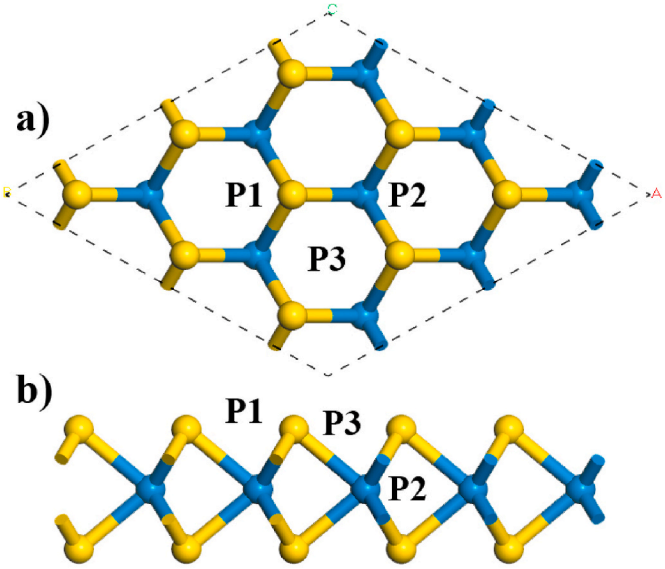

Fig. 1. Views of the optimized WS_2 monolayer (a: top view; b: side view).

Table 1
Detailed adsorption parameters of different gases on monolayer WS_2.

WS_2	*Ea* (eV)	*ΔQ* (e)	*d* (Å)	*r* (Å)
CO	−0.21	0.00	3.46	1.80(C–S)
CO_2	−0.26	0.00	3.33	1.80(C–S)
N_2	−0.21	0.00	3.58	1.77(N–S)
NO	−0.23	0.04	3.20	1.77(N–S)
NO_2	−0.33	−0.03	3.50	1.77(N–S)
O_2	−0.20	0.00	3.55	1.77(O–S)

demonstrate that there is almost no electron localization between monolayer WS_2 and the gas. The undoped monolayer WS_2 does not possess strong gas adsorption capacity, thus it does not have the ability to be a qualified gas sensing material. We can only turn to investigate the gas adsorption performance of the doped monolayer WS_2.

3.3. Adsorption of gas molecules on doped WS_2 monolayer

In this section, we calculate and analyze the adsorption capacity of P-, Si-, Se-, Te- and As-doped monolayer WS_2 for gas molecules (CO, CO_2, N_2, NO, NO_2, O_2).

Firstly, we need to determine whether the structure of each doped substrate is stable. This is a prerequisite for all adsorption calculations. As we observed, the bond lengths of W–S bonds around dopants hardly change, which tells us that doping only changes lengths of W-X bonds. At this point, we can conclude that the adsorption calculations based on each doped substrate are scientific and reliable.

The adsorption parameters of P-, Si-, Se-, Te- and As-doped monolayer WS_2 are listed in Tables S1–4 and Table 2, respectively.

From the perspective of *d*, the adsorption performance of P, Si and As doped monolayer WS_2 for many gases is significantly improved compared with that of pristine monolayer WS_2, while the Se and Te doped monolayer WS_2 are on the contrary. Taking NO_2 adsorption as an example, in the systems doped with P, doped with Si, and doped with As, d decreases from 3.50 Å in the undoped system to 1.91 Å, 1.89 Å and 2.33 Å, respectively; in the Se and Te doped systems, *d* increases to 3.61 Å and 3.68 Å, respectively. From the perspective of *Ea*, the *Ea* of the NO_2/WS_2 system is −0.33 eV. In the systems doped with P, Si, and As, *Ea* grows to −0.88 eV, −2.26 eV and −0.55 eV respectively; while in the Se-doped and Te-doped NO_2 adsorption systems, both *Ea* reduces to −0.28 eV.

Since our goal is to find a 2D material which has the ability to be a qualified NO_2 sensing material, and monolayer WS_2 doped with Se or Te has no advantage in gas adsorption capacity even compared with the undoped monolayer WS_2. Hence, it is obviously not necessary to continue in-depth calculation and analysis for them. Yet at the same time, we also note that the improvement of gas adsorption performance of monolayer WS_2 by Si doping seems to be too comprehensive and significant: in the system doped with Si, in addition to CO_2, when the other five gases (CO, N_2, O_2, NO and NO_2) are adsorbed on Si-doped monolayer WS_2, the *d* (1.82 Å, 1.80 Å, 1.67 Å, 1.89 Å and 1.73 Å) between them and the substrate are less than the corresponding *r* (1.95 Å, 1.92 Å, 1.92 Å, 1.92 Å and 1.92 Å). Whether the selectivity is poor or *d* is too small, it is a disaster for gas sensing materials. A poor selectivity signifies that the gas-sensitive material cannot accurately capture the target gas, and a too small *d* indicates that the gas capture process of the

Table 2
Detailed adsorption parameters of different gases on monolayer As-WS_2.

As-WS_2	*Ea* (eV)	*ΔQ* (e)	*d* (Å)	*r* (Å)
CO	−0.20	0.00	3.59	2.02(C–As)
CO_2	−0.23	−0.01	3.53	2.02(C–As)
N_2	−0.20	0	3.80	1.99(N–As)
NO	−0.62	0.04	2.45	1.99(N–As)
NO_2	−0.55	−0.12	2.33	1.99(N–As)
O_2	−0.19	0.00	3.56	1.99(O–As)

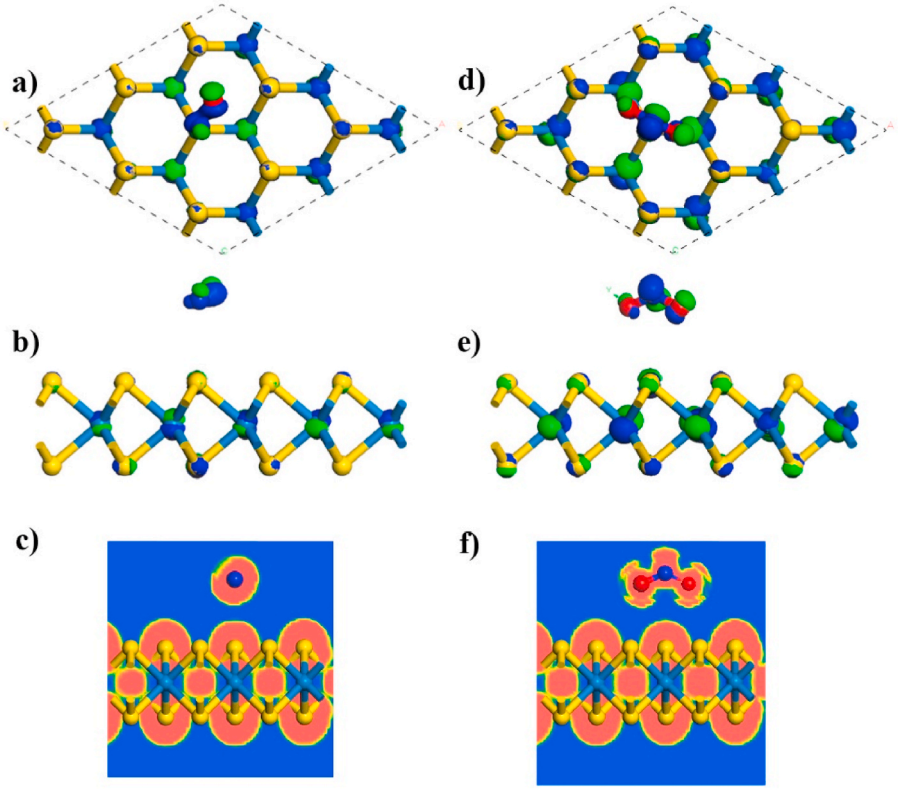

Fig. 2. CDDs of the adsorption systems composed of monolayer WS_2 and NO (a, b) and NO_2 (d, e) (isosurface value: 0.04 e/Å^3) and ELFs of the adsorption systems composed of monolayer WS_2 and NO (c) and NO_2 (f).

gas-sensitive material may not be reversible. In consequence, there is also no need to further explore the possibility of Si-doped monolayer WS_2 as a gas-sensitive material.

Fortunately, P-doping and As-doping enhance the gas adsorption performance of monolayer WS_2 selectively: only when NO and NO_2 are adsorbed on the P-doped or As-doped substrate, are the *d* (1.90 Å, 1.91 Å; 2.45 Å, 2.33 Å) and *r* (1.84 Å, 1.84 Å; 1.99 Å, 1.99 Å) between gas molecules and the substrate relatively close. Like other gases, such as CO_2, *d* is 1.51 Å larger than *r* in both P-doped and As-doped systems, which is not much smaller than the difference of 1.53 Å between *d* and *r* in undoped systems. In addition, in both systems, *d* is not smaller than *r* as in Si-WS_2 systems. Both P-doped and As-doped monolayer WS_2 have the potential to serve as NO_2 sensing materials. Based on the results obtained, we need to perform CDD and ELF calculations on the adsorption system composed of P-doped monolayer WS_2 and NO or NO_2, and the adsorption system composed of As-doped monolayer WS_2 and NO or NO_2, respectively, to reveal the mechanism of interaction between NO or NO_2 and these two doped substrates.

To begin with, the CDD calculation results of each adsorption system are analyzed. From Fig. 3(a–h), in general, we can observe that under the premise of the same isosurface value (all set to 0.04 e/Å^3), compared with As-doped monolayer WS_2 (Fig. 3(e–h)), in the systems which consist of P-doped monolayer WS_2 and two gases (Fig. 3(a–d)), the blue and green regions representing charge accumulation and dissipation are distributed more densely, which is exactly the manifestation of the ΔQ difference between the substrate and the gas in the P-doped and As-doped systems: according to Tables S2 and 2, in the adsorption systems composed of P-WS_2 and NO and NO_2 respectively, the ΔQ between the gas and the substrate is 0.18 e and 0.25 e respectively, which is much greater than the 0.04 e and 0.12 e in As-WS_2 adsorption systems.

Secondly, from the ELF diagram of each adsorption system (Fig. 4 (a–d)), in the interlayer regions between NO and P-WS_2 and between NO_2 and P-WS_2 (Fig. 4(a and b)), the electrons are highly localized, and the red regions representing ELF values of 1 overlap; while in the systems composed of As-WS_2, NO and NO_2 respectively (Fig. 4(c and d)), there are still blue regions representing ELF values of 0 between the substrate and the gas. For ELF, its value ranges from 0 to 1, representing the degree of electron localization from low to high; in the meantime, the degree of electron localization between the substrate and the gas from low to high represents the electron sharing between the substrate and the gas from less to more. It is thereby obvious that there is electron sharing between P-doped monolayer WS_2 and NO and NO_2, and the approach for the doped substrate to adsorb the two gases is chemical adsorption; however, no overlap of electron localization exists between As-doped monolayer WS_2 and NO and NO_2. The As-doped substrate adsorbs both gases by physical adsorption.

Since the P-doped monolayer WS_2 adsorbs NO and NO_2 by chemical adsorption, similar to Si doped monolayer WS_2, the process of capturing NO and NO_2 by P-doped monolayer WS_2 is not reversible; and since the

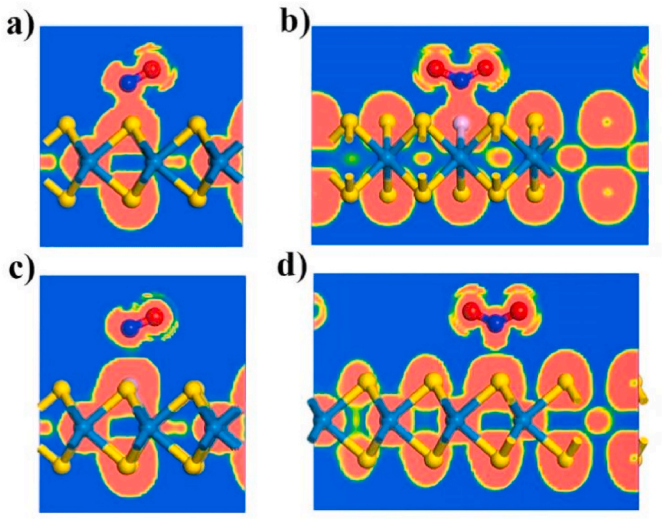

Fig. 4. ELFs of the adsorption systems composed of P-doped monolayer WS_2 and NO (a) and NO_2 (b) and the adsorption systems composed of As-doped monolayer WS_2 and NO (c) and NO_2 (d).

As-doped monolayer WS_2 adsorbs NO and NO_2 in a physical way, thus by increasing the ambient temperature or applying an external electric field, without destroying the structure of the As-doped monolayer WS_2, the NO and NO_2 adsorbed by As-doped monolayer WS_2 can be restored to a free state, and in other words, the process of capturing NO and NO_2 by As-doped monolayer WS_2 is reversible.

And because, in the adsorption systems which consist of As-WS_2, NO and NO_2, the ΔQ is 0.04 e and 0.12 e, respectively. Apparently, compared with NO_2, ΔQ between NO and As-WS_2 is too small. Although As-doped monolayer WS_2 adsorbs NO and NO_2 by physical adsorption, it must be considered that too small ΔQ leads to too small electrical signal change before and after the sensing material adsorbs gas, that is so say, as a result, the As-doped monolayer WS_2 has little discrimination before and after the adsorption of NO. Therefore, As-doped monolayer WS_2 is a 2D material that is more qualified as a NO_2-sensitive material, which is in line with our goal.

3.4. Optical properties

The behavior of adsorption will change the properties of materials, which is vividly reflected in optical properties [54,55]. By observing the optical properties of As-doped adsorption systems, the gas adsorption can be studied more clearly and the feasibility of the practical application of NO_2 gas sensor based on monolayer As-WS_2 can be further elaborated.

The complex refractive index represents the difference between

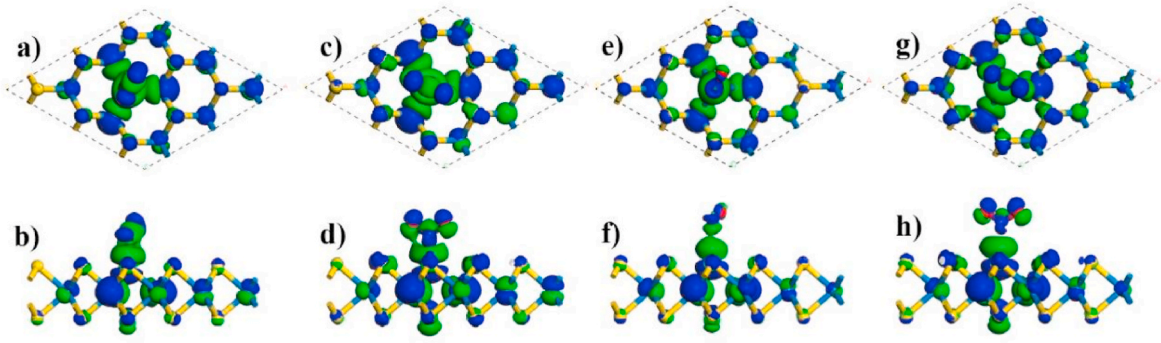

Fig. 3. CDDs of the adsorption systems composed of P-doped monolayer WS_2 and NO (a, b) and NO_2 (c, d) and the adsorption systems composed of As-doped monolayer WS_2 and NO (e, f) and NO_2 (g, h) (isosurface value: 0.04 e/Å^3).

electromagnetic waves propagating in vacuum and other materials, which is represented by real and imaginary parts, respectively [56]:

$$N = n + ik \tag{3}$$

Other relevant optical properties can also be calculated from the real and imaginary parts of the complex refractive index. Among them, the complex dielectric function is a vital optical parameter, which stands for the process of electron transition. Its real part and imaginary parts have different meanings, which correspond to the process of absorbing and releasing photons, respectively [57]. Their expressions are [58,59]:

$$\varepsilon = \varepsilon_1 + \varepsilon_2 \tag{4}$$

$$\varepsilon_1 = n^2 - k^2 \tag{5}$$

$$\varepsilon_2 = 2nk \tag{6}$$

Due to the correlation between optical properties, reflectivity (especially in the simple case of perpendicular incidence to the plane) can also be obtained from the complex refractive index [59]:

$$R = \left|\frac{1-N}{1+N}\right|^2 = \frac{(n-1)^2 + k^2}{(n+1)^2 + k^2} \tag{7}$$

Fig. 5(a) demonstrates the imaginary part of the dielectric function before and after As-doped monolayer WS_2 adsorbs NO_2 gas. In the entire visible region, both systems have function values greater than zero. The difference is that in the region between 390 and 670 nm, the function value of the system before adsorption of NO_2 is higher than that of the system after adsorption of NO_2. When the wavelength of light exceeds 670 nm, the opposite happens. This means that in the visible region, the As-WS_2 system has a higher utilization rate of visible light than the adsorption system composed of As-doped monolayer WS_2 and NO_2 [52].

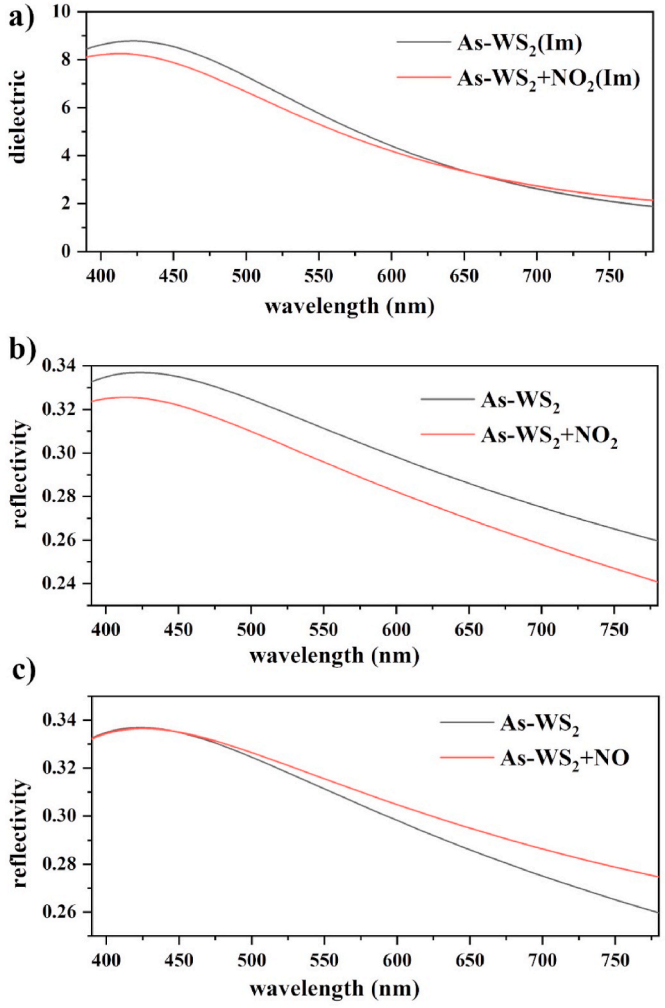

Fig. 5. The imaginary part of the dielectric function of NO_2/As-doped monolayer WS_2 system (a) and the reflectivity of NO_2/As-doped monolayer WS_2 system (b) and NO/As-doped monolayer WS_2 system (c).

Also, from Fig. 5(b and c), with the increase of the wavelength of light, the reflectivity of the two systems first reaches an insignificant peak at about 470 nm and then decreases all the time. For the adsorption system composed of As-doped monolayer WS_2 and NO_2, its reflectivity is always lower than that of the monolayer As-WS_2 system itself in the entire visible region (Fig. 5(b)); and for the adsorption system composed of As-doped monolayer WS_2 and NO, the variation of reflectivity before and after monolayer As-WS_2 adsorbs NO is not obvious (Fig. 5(c)), especially in the interval from 390 to 500 nm, the two are almost identical. This allows us to understand that when monolayer As-WS_2 is used as a sensing material for NO_2, such a difference in reflectivity can make its state more conveniently judged.

Through the above analysis, conclusion is reached that the difference in optical properties before and after monolayer As-WS_2 adsorbs NO_2 gas can be safely used to help determine whether NO_2 gas is absorbed by monolayer As-WS_2, so that the accuracy of NO_2 gas sensors based on monolayer As-WS_2 can be improved under certain circumstances.

3.5. Recovery time

Recovery time is another vital parameter to measure whether the sensing material has practicality or not. Here, the recovery time of the adsorption system composed of As-doped monolayer WS_2 and NO_2 is calculated. The transition state theory enlightens us that the recovery time can be estimated via the following equation [60]:

$$\tau = w^{-1} e^{\frac{-E^*}{kT}} \tag{8}$$

where T is the temperature, k corresponds to the Boltzmann constant, w represents the trial frequency (10^{13} s^{-1}) [61], and E^* stands for the desorption energy barrier, which is numerically equal to Ea [62].

It can be seen from this formula that with temperature increasing, the recovery time will become smaller and smaller. Therefore, the increase in temperature can increase the possibility of repeated use of the sensor. Several temperature values, namely T = 200 K, 300 K and 1000 K, are selected for the calculation of the recovery time of As-doped monolayer WS_2 after it adsorbs NO_2 gas, respectively. At 200 K, the recovery time of the NO_2 adsorption system is 6.927 s; at 300 K, it falls to 0.169 ms; and at 1000 K, it drops to only 34.37 ns. It can be seen from the different recovery times corresponding to different temperatures that the increase in temperature makes it easier for NO_2 to leave the surface of the substrate. Not only that, it can be discovered that even at a very low atmospheric temperature (200 K), the desorption time is still an ideal value. As-doped monolayer WS_2 is thereby further verified as an ideal NO_2 sensing material.

3.6. DOS and PDOS

Last but not least, in order to fully illustrate the high sensitivity of monolayer As-WS_2 to NO_2 molecules and the persuasiveness of previous results, the DOS and PDOS of the system composed of As-doped monolayer WS_2 and NO_2 are calculated.

The DOS curves of the As-WS_2 system before and after the adsorption of NO_2 are compared (Fig. 6(a and b)). It can be seen from Fig. 6(a) that the curve before and after adsorption has shifted, and new absorption peaks (at approximately 1 eV) also appear. If the DOS curve before and after adsorption changes significantly (mainly reflected in the overall displacement of the curve or the appearance of new peaks), then the substrate has a high sensitivity to gas molecules.

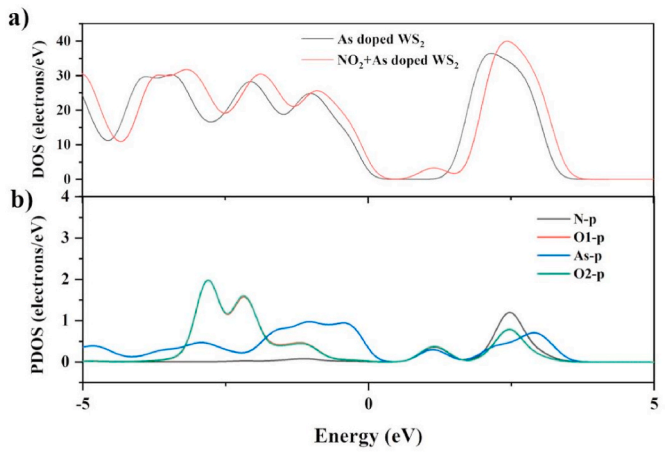

Fig. 6. DOS (a) and PDOS (b) of the adsorption systems composed of As-doped monolayer WS_2 and NO_2.

Then, since there is only p-type hybridization between As and NO_2, as shown in Fig. 6(b) only the PDOS of the p-orbitals of the dopant atom As and the N, O1 and O2 atoms of the adsorbed gas NO_2 are calculated. It can be observed that from −5 eV to 5 eV, the PDOS curves of the p-orbitals of these four atoms do have similar variation trends. If the same trends on the PDOS curves of the dopant atom and the atom closest to it in the adsorbed gas molecule are observed at a specific energy, then orbital hybridization exists between the two atoms. This phenomenon can be explained as a strong interaction between the substrate and the gas.

Through above analysis, As-doped monolayer WS_2 can indeed be considered as having sufficient sensitivity to NO_2. In a nutshell, As-WS_2 monolayer is a strong candidate for NO_2 sensing materials.

4. Conclusion

In this paper, through DFT calculation and comparison of the changes of ΔQ, CDD, ELF, optical properties, recovery time, DOS and PDOS and other related properties before and after the pristine and doped (Si, P, Se, Te, As) monolayer WS_2 adsorb gases (CO, CO_2, N_2, NO, NO_2, O_2), the possibility of As-doped monolayer WS_2 as a NO_2-sensitive material is explored and determined. Through the comparison among adsorption distances, both P-WS_2 and As-WS_2 are shown to have the possibility of being NO and NO_2 sensors. Through the calculation of CDD and ELF, it is found that P-WS_2 adsorbs both NO and NO_2 in a chemical way. Between the remaining two adsorption systems, NO_2/As-WS_2 system is superior to NO/As-WS_2 system in charge transfer and reflectivity. Also, the calculation of recovery time helps us understand that the recovery time of NO_2/As-WS_2 system is still within an acceptable range even at a very low atmospheric temperature. PDOS and DOS analysis also verify that monolayer As-WS_2 is a promising substrate material for NO_2 sensors.

Credit author statement

Shuhan Hou: Conceptualization, Methodology, Software, Writing – original draft preparation, Reviewing and Editing. Zhaokun Wang: Methodology, Data curation, Software, Visualization, Validation, Reviewing and Editing. Huiru Yang: Methodology, Software, Investigation. Jing Jiang: Data curation, Investigation. Chenshan Gao: Methodology, Software, Investigation. Yufei Liu: Visualization, Investigation. Xiaosheng Tang: Visualization, Investigation. Huaiyu Ye: Conceptualization.

Declaration of competing interest

The authors declare that they have no known competing financial interests or personal relationships that could have appeared to influence the work reported in this paper.

Acknowledge

This work was supported by the National Key R&D Program of China (2018YFE0204600), the Shenzhen Fundamental Research Program (JCYJ20200109140822796), and the NSQKJJ under grant K21799119.

Appendix A. Supplementary data

Supplementary data to this article can be found online at https://doi.org/10.1016/j.physe.2022.115446.

References

[1] M. Ikram, L. Liu, Y. Liu, L. Ma, H. Lv, M. Ullah, L. He, H. Wu, R. Wang, K. Shi, Fabrication and characterization of a high-surface area MoS2@WS2 heterojunction for the ultra-sensitive NO2 detection at room temperatureElectronic supplementary information (ESI) available. See, J. Mater. Chem. A, Mater. Energy Sustain. 7 (2019) 1462–14612, https://doi.org/10.1039/c9ta03452h.
[2] M. Dorado, Exhaust emissions from a Diesel engine fueled with transesterified waste olive oil, Fuel 82 (2003) 1311–1315.
[3] Z. Hong, Z. Wang, X. Li, Catalytic oxidation of nitric oxide (NO) over different catalysts: an overview, Catal. Sci. Technol. 7 (2017) 3440–3452.
[4] G. Neri, First fifty years of chemoresistive gas sensors, Chemosensors 3 (2015) 1–20.
[5] A. Vergara, K.D. Benkstein, C.B. Montgomery, S. Semancik, Demonstration of fast and accurate discrimination and quantification of chemically similar species utilizing a single cross-selective chemiresistor, Anal. Chem. 86 (2014) 6753–6757.
[6] C. Wang, X. Cui, J. Liu, X. Zhou, X. Cheng, P. Sun, X. Hu, X. Li, J. Zheng, G. Lu, Design of superior ethanol gas sensor based on Al-doped NiO nanorod-flowers, ACS Sens. 1 (2015) 131–136.
[7] W. Yang, L. Gan, H. Li, T. Zhai, Two-dimensional layered nanomaterials for gas-sensing applications, Inorg. Chem. Front. 3 (2016) 433–451.
[8] Q. Yue, Z. Shao, S. Chang, J. Li, Adsorption of gas molecules on monolayer MoS2 and effect of applied electric field, Nanoscale Res. Lett. 8 (2013) 1–7.
[9] E.W. Keong Koh, C.H. Chiu, Y.K. Lim, Y.-W. Zhang, H. Pan, Hydrogen adsorption on and diffusion through MoS2 monolayer: first-principles study, Int. J. Hydrogen Energy 37 (2012) 14323–14328.
[10] C. Zhou, W. Yang, H. Zhu, Mechanism of charge transfer and its impacts on Fermi-level pinning for gas molecules adsorbed on monolayer WS2, J. Chem. Phys. 142 (2015), 214704.
[11] D. Zhang, J. Wu, P. Li, Y. Cao, Room-temperature SO2 gas-sensing properties based on a metal-doped MoS2 nanoflower: an experimental and density functional theory investigation, J. Mater. Chem. A, Mater. Energy Sustain. 5 (2017) 2666–2677.
[12] X. Li, X. Li, Z. Li, J. Wang, J. Zhang, WS2 nanoflakes based selective ammonia sensors at room temperature, Sensor. Actuator. B Chem. 240 (2017) 273–277.
[13] A.K. Geim, K.S. Novoselov, The rise of graphene, Nat. Mater. 6 (2007) 183–191.
[14] K. Cheah, M. Forsyth, V.T. Truong, Ordering and stability in conducting polypyrrole, Synth. Met. 94 (1998) 215–219.
[15] C. Anichini, W. Czepa, D. Pakulski, A. Aliprandi, A. Ciesielski, P. Samori, Chemical sensing with 2D materials, Chem. Soc. Rev. 47 (2018) 4860–4908.
[16] M.S. Pawar, D.J. Late, Temperature-dependent Raman spectroscopy and sensor applications of PtSe2 nanosheets synthesized by wet chemistry, Beilstein J. Nanotechnol. 10 (2019) 467–474.
[17] D. Chen, X. Zhang, J. Tang, Z. Cui, H. Cui, S. Pi, Theoretical study of monolayer PtSe2 as outstanding gas sensor to detect SF6 decompositions, IEEE Electron. Device Lett. 39 (2018) 1405–1408.
[18] X. Liu, T. Ma, N. Pinna, J. Zhang, Two-dimensional nanostructured materials for gas sensing, Adv. Funct. Mater. 27 (2017).
[19] B.L. Li, J. Wang, H.L. Zou, S. Garaj, C.T. Lim, J. Xie, N.B. Li, D.T. Leong, Low-dimensional transition metal dichalcogenide nanostructures based sensors, Adv. Funct. Mater. 26 (2016) 7034–7056.
[20] H. Wang, L. Yu, Y.-H. Lee, Y. Shi, A. Hsu, M.L. Chin, L.-J. Li, M. Dubey, J. Kong, T. Palacios, Integrated circuits based on bilayer MoS2 transistors, Nano Lett. 12 (2012) 4674–4680.
[21] W. Wei, Y. Dai, B. Huang, In-plane interfacing effects of two-dimensional transition-metal dichalcogenide heterostructures, Phys. Chem. Chem. Phys. 18 (2016) 15632–15638.
[22] T.H. Kim, Y.H. Kim, S.Y. Park, S.Y. Kim, H.W. Jang, Two-dimensional transition metal disulfides for chemoresistive gas sensing: perspective and challenges, Chemosensors 5 (2017) 15.
[23] G. Neri, Thin 2D: the new dimensionality in gas sensing, Chemosensors 5 (2017) 21.
[24] F.K. Perkins, A.L. Friedman, E. Cobas, P.M. Campbell, G.G. Jernigan, B.T. Jonker, Chemical vapor sensing with monolayer MoS2, Nano Lett. 13 (2013) 668–673.

[25] B. Cho, M.G. Hahm, M. Choi, J. Yoon, A.R. Kim, Y.-J. Lee, S.-G. Park, J.-D. Kwon, C. S. Kim, M. Song, Y. Jeong, K.-S. Nam, S. Lee, T.J. Yoo, C.G. Kang, B.H. Lee, H.C. Ko, P.M. Ajayan, D.-H. Kim, Charge-transfer-based gas sensing using atomic-layer MoS2, Sci. Rep. 5 (2015) 8052, 8052.
[26] D.J. Late, Y.-K. Huang, B. Liu, J. Acharya, S.N. Shirodkar, J. Luo, A. Yan, D. Charles, U.V. Waghmare, V.P. Dravid, C.N.R. Rao, Sensing behavior of atomically thin-layered MoS2 transistors, ACS Nano 7 (2013) 4879–4891.
[27] Q.H. Wang, K. Kalantar-Zadeh, A. Kis, J.N. Coleman, M.S. Strano, Electronics and optoelectronics of two-dimensional transition metal dichalcogenides, Nat. Nanotechnol. 7 (2012) 699–712.
[28] K.Y. Ko, J.-G. Song, Y. Kim, T. Choi, S. Shin, C.W. Lee, K. Lee, J. Koo, H. Lee, J. Kim, T. Lee, J. Park, H. Kim, Improvement of gas-sensing performance of large-area tungsten disulfide nanosheets by surface functionalization, ACS Nano 10 (2016) 9287–9296.
[29] M. O'Brien, K. Lee, R. Morrish, N.C. Berner, N. McEvoy, C.A. Wolden, G. S. Duesberg, Plasma assisted synthesis of WS2 for gas sensing applications, Chem. Phys. Lett. 615 (2014) 6–10.
[30] H. Li, Z. Yin, Q. He, H. Li, X. Huang, G. Lu, D.W.H. Fam, A.I.Y. Tok, Q. Zhang, H. Zhang, Fabrication of single- and multilayer MoS2 film-based field-effect transistors for sensing NO at room temperature, Small 8 (2012) 63–67.
[31] Q. He, Z. Zeng, Z. Yin, H. Li, S. Wu, X. Huang, H. Zhang, Fabrication of flexible MoS2 thin-film transistor arrays for practical gas-sensing applications, Small 8 (2012) 2994–2999.
[32] L. Hao, Y. Liu, Y. Du, Z. Chen, Z. Han, Z. Xu, J. Zhu, Highly enhanced H 2 sensing performance of few-layer MoS 2/SiO 2/Si heterojunctions by surface decoration of Pd nanoparticles, Nanoscale Res. Lett. 12 (2017) 567.
[33] R. Kumar, P.K. Kulriya, M. Mishra, F. Singh, G. Gupta, M. Kumar, Highly selective and reversible NO2 gas sensor using vertically aligned MoS2 flake networks, Nanotechnology 29 (2018) 464001, 464001.
[34] S. Sharma, A. Kumar, D. Kaur, Room Temperature Ammonia Gas Sensing Properties of MoS2 Nanostructured Thin Film, (in).
[35] V.Q. Bui, T.-T. Pham, D.A. Le, C.M. Thi, H.M. Le, A first-principles investigation of various gas (CO, H2O, NO, and O2) absorptions on a WS2 monolayer: stability and electronic properties, J. Phys. Condens. Matter 27 (2015) 305005, 305005.
[36] D.-R. Hang, D.-Y. Sun, C.-H. Chen, H.-F. Wu, M.M.C. Chou, S.E. Islam, K.H. Sharma, Facile bottom-up preparation of WS2-based water-soluble quantum dots as luminescent probes for hydrogen peroxide and glucose, Nanoscale Res. Lett. 14 (2019) 1–15.
[37] C. Zhou, W. Yang, H. Zhu, Mechanism of charge transfer and its impacts on Fermi-level pinning for gas molecules adsorbed on monolayer WS2, J. Chem. Phys. 142 (2015) 214704, 214704.
[38] J. Cao, J. Zhou, Y. Zhang, X. Liu, Theoretical study of H.sub.2 adsorbed on monolayer MoS.sub.2 doped with N, Si, P, Microelectron. Eng. 190 (2018) 63.
[39] O. Faye, J.A. Szpunar, B. Szpunar, A.C. Beye, Hydrogen adsorption and storage on Palladium – functionalized graphene with NH-dopant: a first principles calculation, Appl. Surf. Sci. 392 (2017) 362–374.
[40] W.T. Koo, J.H. Cha, J.W. Jung, S.J. Choi, J.S. Jang, D.H. Kim, I.D. Kim, Gas sensors: few-layered WS2 nanoplates confined in Co, N-doped hollow carbon nanocages: abundant WS2 edges for highly sensitive gas sensors (adv. Funct. Mater. 36/2018), Adv. Funct. Mater. 28 (2018) 1870254–n/a.
[41] C. Kuru, D. Choi, A. Kargar, C.H. Liu, S. Yavuz, C. Choi, S. Jin, P.R. Bandaru, High-performance flexible hydrogen sensor made of WS2 nanosheet-Pd nanoparticle composite film, Nanotechnology 27 (2016) 195501, 195501.
[42] A. Abbasi, A. Abdelrasoul, J.J. Sardroodi, Adsorption of CO and NO molecules on Al, P and Si embedded MoS.sub.2 nanosheets investigated by DFT calculations, Adsorption, J. Int. Adsorp. Soc. 25 (2019).
[43] M.D. Esrafili, S. Heydari, NO reduction over an Al-embedded MoS2 monolayer: a first-principles studyElectronic supplementary information (ESI) available, RSC Adv. 9 (2019) 38973–38981, https://doi.org/10.1039/c9ra05759e. See.
[44] D. Li, W. Li, J. Zhang, Al doped MoS.sub.2 monolayer: a promising low-cost single atom catalyst for CO oxidation, Appl. Surf. Sci. 484 (2019) 1297.
[45] S. Zhang, Z. Li, J. Li, G. Hao, C. He, T. Ouyang, C. Zhang, C. Tang, J. Zhong, Strain effects on magnetic states of monolayer MoS2 doped with group IIIA to VA atoms, Phys. E Low-dimens. Syst. Nanostruct. 114 (2019), 113609.
[46] C.M. Marian, A. Heil, M. Kleinschmidt, The DFT/MRCI method, Wiley interdisciplinary reviews, Comput. Mol. Sci. 9 (2019) n/a.
[47] S. Seyyed Amir, R. Solmaz, Switching behavior of an actuator containing germanium, silicon-decorated and normal C20 fullerene, Chem. Rev. Lett. 1 (2018) 77–81.
[48] S. Mohammad Reza Jalali, A. Roya, R. Behnam Farhang, Procarbazine adsorption on the surface of single walled carbon nanotube: DFT studies, Chem. Rev. Lett. 3 (2020) 175–179.
[49] J.P. Perdew, K. Burke, M. Ernzerhof, Generalized gradient approximation made simple, Phys. Rev. Lett. 77 (1996) 3865–3868.
[50] N. Mardirossian, M. Head-Gordon, ωB97X-V: a 10-parameter, range-separated hybrid, generalized gradient approximation density functional with nonlocal correlation, designed by a survival-of-the-fittest strategy, Phys. Chem. Chem. Phys. : Phys. Chem. Chem. Phys. 16 (2014) 994–9924.
[51] R.M. Irelan, T.M. Henderson, G.E. Scuseria, Long-range-corrected hybrids using a range-separated Perdew-Burke-Ernzerhof functional and random phase approximation correlation, J. Chem. Phys. 135 (2011), 094105-094105-094107.
[52] S. Grimme, Semiempirical GGA-type density functional constructed with a long-range dispersion correction, J. Comput. Chem. 27 (2006) 1787–1799.
[53] M. Mohan, V.K. Singh, S. Reshmi, S.R. Barman, K. Bhattacharjee, Atomic adsorption of Sn on mechanically cleaved WS2 surface at room temperature, Surf. Sci. 701 (2020), 121685.
[54] P. Gao, L. Yang, S. Xiao, L. Wang, W. Guo, J. Lu, Effect of Ru, Rh, Mo, and Pd adsorption on the electronic and optical properties of anatase TiO2(101): a DFT investigation, Materials 12 (2019) 814.
[55] M. Ito, Y. Ito, D. Nii, H. Kato, K. Umemura, Y. Homma, The effect of DNA adsorption on optical transitions in single walled carbon nanotubes, J. Phys. Chem. C 119 (2015) 21141–21145.
[56] X. Li, Y. Wu, D. Gu, F. Gan, Spectral, thermal and optical properties of metal(II)–azo complexes for optical recording media, Dyes Pigments 86 (2010) 182–189.
[57] S. Fei, Q. Feng, Y. Chen, X. Bai, H. Zhu, Effect of surface oxidation on optical CO gas-sensing characteristics of N/Rh-codoped rutile TiO2, Zhongguo Jiguang 46 (2019), 1103003.
[58] P. Aryal, A.-R. Ibdah, P. Pradhan, D. Attygalle, P. Koirala, N.J. Podraza, S. Marsillac, R.W. Collins, J. Li, Parameterized complex dielectric functions of CuIn1−xGaxSe2: applications in optical characterization of compositional non-uniformities and depth profiles in materials and solar cells, Prog. Photovolt. 24 (2016) 1200–1213.
[59] E.D. Palik, Handbook of Optical Constants of Solids, Elsevier Science & Technology, San Diego, 1998.
[60] A. Kokalj, Formation and structure of inhibitive molecular film of imidazole on iron surface, Corrosion Sci. 68 (2013) 195–203.
[61] S. Weigelt, C. Busse, C. Bombis, M.M. Knudsen, K.V. Gothelf, T. Strunskus, C. Wöll, M. Dahlbom, B. Hammer, E. Lægsgaard, F. Besenbacher, T.R. Linderoth, Covalent interlinking of an aldehyde and an amine on a Au(111) surface in ultrahigh vacuum, Angew. Chem. 119 (2007) 9387–9390.
[62] H. Yang, Z. Wang, H. Ye, K. Zhang, X. Chen, G. Zhang, Promoting sensitivity and selectivity of HCHO sensor based on strained InP3 monolayer: a DFT study, Appl. Surf. Sci. 459 (2018) 554–561.